Chemistry Research Journal, 2017, 2(5):15-21

Available online www.chemrj.org

Research Article

ISSN: 2455-8990
CODEN(USA): CRJHA5

Relationship between Band gap and particle size of Cadmium sulfide Quantum Dots

N. E. Makori*[1], Duke Ayetah Oeba[1], Cliff Orori Mosiori[2]

[1]Department of Physics, Kenyatta University, P.O. Box 43844 - 00100, Nairobi
[2]Department of Mathematics and Physics, Technical University of Mombasa, P.O. Box 90420- 80100, Mombasa

Abstract Nanoparticles at quantum dot level are considered to be larger than individual atoms and molecules but smaller than their bulk solid. In such a condition, they are believed to obey neither absolute quantum chemistry nor laws of classical physics. Therefore they have properties that differ significantly from those expected experimentally. Therefore, there are two major phenomena observed that are responsible for these differences. The first one is the high dispersity of nanocrystalline systems or quantum dots. Its acceptable that as the size of a quantum dot is reduced, the number of dots at the surface of the crystal compared to the number of atoms in the crystal itself, increases and therefore the properties, which are usually determined by the molecular structure of the bulk lattice, now become increasingly dominated by the defect structure of the surface. The main objective of this study was to use synthetic method to prepare certain types of nanoparticles and study the difference in properties between bulk and nanosize semiconducting nanoparticles. Absorbance measurements were collected from the UV-Vis spectrum and used in conjunction with Beer-Lambert's Law to calculate concentrations of solutions or the absorbance coefficient ε . Equation required the band gap energy of the nanoparticles were obtained from the UV-Vis results and used to calculate the energy absorbed by a quantum dot.

Keywords Quantum dots, CdS, Naanoparticles, spectroscopic technique, Band Gap, Absorbance

1. Introduction

The UV-Vis spectrometry is a spectroscopic technique involving the use of light in the visible, near ultra-violet and near infrared regions to cause electronic transitions in the target material. It uses a light source of a fixed wavelength that is shone through a sample and its absorption intensity is measured against a background using a detector. The wavelength is then varied slightly using perhaps a diffractometer, and the process repeated until the absorption ratio for a spectrum of wavelengths is obtained. UV-Visible spectrometry is instrumental in characterizing quantum dots to determine their band gap energy as well as their particle sizes. The band gap of a material is defined as the energy distance between the valence and conduction bands. The smaller the band gap, the more electrically conductive a material will be. One can add dopants to semiconductors like cadmium sulfide quantum dots which make a semiconductor behave more like a conductor by introducing additional energy levels within the band gap. A quantum dots can be defined as a nanoscale particle of semiconducting material that can be embedded in cells or organisms for various experimental purposes, such as labeling proteins. Quantum confinement is defined as a confining of the movement of the particles in one or more dimensions. Quantum dots can are regarded as semiconductors who excitons experience quantum confinement in all three spatial dimensions. The confinement causes their properties to lie between those of bulk semiconductors and those of discrete molecules since this

confinement alters opto-electrical properties of these dots. Such alteration in properties can be exploited for applications in transistors, light-emitting diodes, diode lasers, and photovoltaic devices. Quantum confinement properties may be exploited to produce very precise optical emissions when excited with energetic electrons or photons leading to such new devices as quantum LEDs, nanocrystal solar cells, and programmable matter. Quantum dots have the characteristic property of being able to respond to very fast changes in incoming energy quantities. Therefore, cadmium sulfide quantum dots in particular have exhibit different optical and electrical properties from its bulk material for such applications. This makes them well suited to nascent areas of research such as wave guides, high speed optical switches, and fast response resonators.

2. Theoretical Concepts

All molecules have orbitals that are formed by a adding or subtracting their corresponding atomic orbitals known as bonding and antibonding orbitals. The bonding orbital is known as the highest occupied molecular orbital (HOMO) and contains the valence electrons. The antibonding orbital, is known as the lowest occupied molecular orbital (LUMO) and is normally devoid of electrons. It's clear that electrons in the valence band are tightly coupled with their respective nuclei, whereas electrons in the conduction band are somewhat separated from their respective nuclei therefore allowing for free motion within the solid. When these dimensions are comparable to the de Broglie wavelength of the particle, quantum confinement effects take place and cause the band gap of the particle to increase. Bulk solids are a composition of several thousands of atoms which contribute to highly overlapping orbitals leading to less pronounced energy bands and consequently a smaller band gap. Therefore to determine the band gap, we consider;

$$E_g^* = E_g^{bulk} + \frac{\hbar^2\pi^2}{2r^2}\left(\frac{1}{m_e^*}+\frac{1}{m_h^*}\right) - \frac{1.8e^2}{4\pi\varepsilon\,\varepsilon_0 r} - \frac{0.124e^4}{\hbar^2(4\pi\varepsilon\,\varepsilon_0)^2}\left(\frac{1}{m_e^*}+\frac{1}{m_h^*}\right)^{-1} \quad (1)$$

where, $E_g^* =$ = band gap energy, $E_g^{Bulk} =$ = band gap energy of the bulk (value of 3.88×10^{-19} J); h = Planck's Constant, 6.625×10^{-34} J·s; r = particle radius (m); m_e = mass of a free electron, 9.11×10^{-31} kg; m_e^* = $0.19m_e$ (*effective mass of a conduction band electron in CdS*); $m_h^* = 0.80m_e$ (*effective mass of a valence band hole in CdS*); *e* = elementary charge, 1.602×10^{-19}C; $\varepsilon_0 = 8.854\times10^{-12}\text{C}^2\text{N}^{-1}\text{m}^{-2}$ (*permittivity of free space);* ε = 5.7 (*relative permittivity of CdS*). Using Eq. (1), the cut-off wavelength is obtained from the intersection of the tangent line of the peak with the wavelength axis leading to the band gap E_g^* of:

$$E_g^* = \frac{hc}{\lambda_c} \quad (2)$$

where λ_c = wavelength absorbed, and *c* is the speed of light, Therefore using Eq. (2), the size of a particle is derived from the effective mass model:

$$E_g^* = E_g^{bulk} + \frac{\bar{h}^2\pi^2}{2r^2}\left(\frac{1}{m_e^*}+\frac{1}{m_h^*}\right) - \frac{1.8e^2}{4\pi\varepsilon\varepsilon_0 r} - \frac{0.124e^4}{\bar{h}^2(4\pi\varepsilon\varepsilon_0)^2}\left(\frac{1}{m_e^*}+\frac{1}{m_h^*}\right)^{-1} \quad (3)$$

3. Methodology

3.1. Materials and Chemicals

AOT/n-heptane solution and sources of Cd^{2+} and S^{2-} solutions were obtained among other laboratory apparatus and reagents.

3.2. Preparation of CdS quantum dots

Samples of CdS quantum dots were prepared using the inverted-micelle synthesis. They were purified, and were subsequently analyzed by UV-Vis spectroscopy as follows: The AOT/n-heptane solution was prepared prior to the

experiment. The solution with CdS quantum dots was evaporated under a Schlenk line. It was then washed with n-heptane and dried again under vacuum severally. Finally, the last centrifuge at 10 000 rpm for 2 minutes was bypassed. After stirring the micelle solutions for 20 minutes, the solution remained transparent. When 0.25 mL of both Cd^{2+} and S^{2-} were added, the solution gave a yellow colour.

4. Results and Discussion

4.1. UV-Vis Spectrometric Analysis

The UV-Vis measurement was performed on a UV-Vis spectrometer. The light source is varied in wavelength to give the UV-Vis spectrum of the sample. The set up can be represented by the schematic figure 1 in which a sample is exposed to light that passed through a monochromator and aperture, detected, and analyzed.

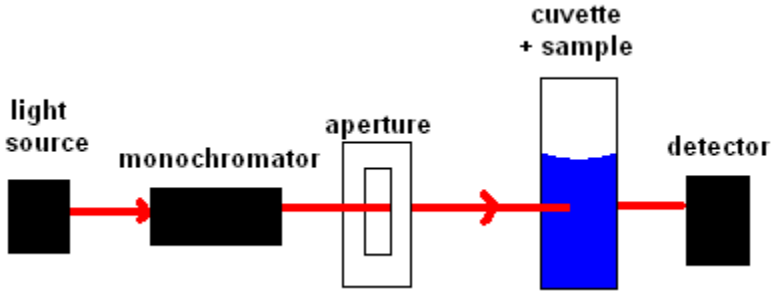

Figure 1: Basic schematic of a UV-Vis spectrometer

The obtained spectrum was very similar to CdS in most literature [2, 6, 12, 14, 15]. However the drop between 375 and 450 nm is typical for nano-sized particles of CdS as compared to that observed in [4], where the CdS quantum dot sample was prepared by a thin-film latex method where it showed an absorbance drop between 250 and 400 nm, as opposed to their bulk sample which had the drop between 500 and 600 nm. The particle size of the sample from [13] was predicted to be 7.6 nm.

4.2. Qualitative Analysis

4.2.1. Absorbance Spectra

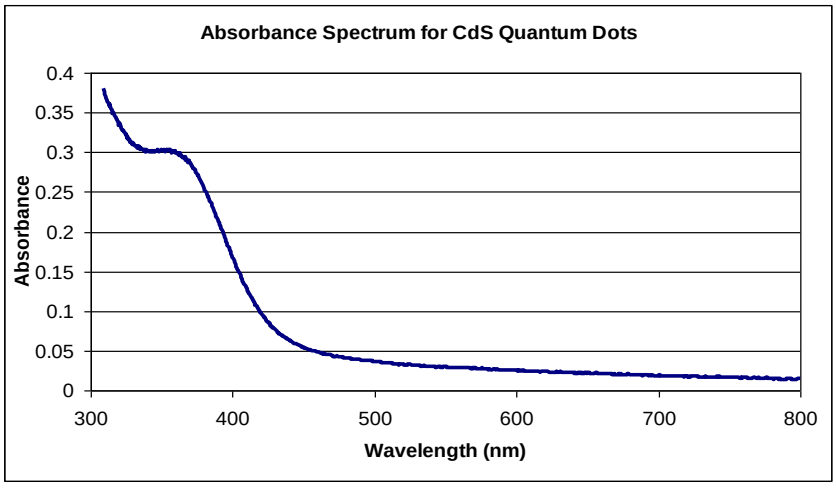

Figure 2: Noise free -UV-Vis Absorbance Spectrum for CdS Quantum Dots

The UV-Vis Absorbance Spectrum for CdS Quantum Dots with noisy range removed was plotted in figure 2. As portrayed by the curve in figure 2, it can be noted that below a wavelength of 300 nm, the spectrum is very noisy, though a clean signal at energies below this point is evident. However, the only feature present in the spectrum is a dip from 0.3, to around 0, in the range of 375 to 450 nm wavelength. Therefore beyond this point as depicted by the curve, the absorbance is essentially zero. Equally, there are no small peaks or dips anywhere in the whole spectrum.

When this spectrum is closely compared with similar studies, the pattern is similar to the literature on UV-Vis on bulk CdS, except that for bulk, the drop in absorbance occurs between 500 and 600 nm, such as in [2] and [3].
Such a shift is expected theoretically [4], as a smaller particle size means a larger band gap, since fewer molecular orbitals are being added to the possible energy states of the particle. Hence, absorption will occur at higher energies, so a shift towards shorter wavelengths will be apparent.

4.2.2. Band Gap Measurement

Band gap was important factor that was measured [7]. The band gap of the particles in this experiment was measured to be 2.821 eV, whereas in bulk, the value is 2.45 eV [11]. Based on these figures, a higher band gap was observed at a lower particle size. This is consistent and in agreement with the shift of the drop on the UV-Vis spectrum. Lower band gap observed in this study was for a smaller particle size as expected by theory just as reported by literature in [6] reports a very small particle size of 1 nm for CdS, and in [12] which gave a band gap 3.9 eV. Hence, this trend is consistent with the literature. The excel software application was used to determine the band gap. A line of best fit was drawn for the linear portion near the peak in the spectrum, as shown in figure 4, in which the line is as shown in figure 2, along with an R^2 value near 1 to confirm that this portion is linear. The critical wavelength was determined to be equal to 435.9 nm. Using this value and Eq. (1), the band gap was calculated to be 2.82 eV and using Eq. (3), the particle size was calculated as 3.8 nm. The band gap was accurate to 3 significant figures, based on the wavelength and absorbance values provided by the UV-Vis spectrometer while the calculated particle size was accurate only to two significant figures based on the used effective mass of electrons and holes values in CdS [10].

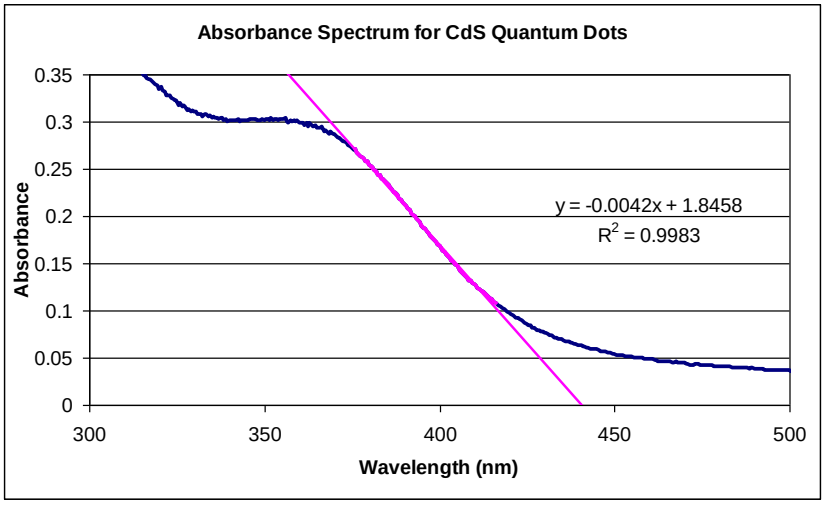

Figure 3: Linear region of UV-Vis spectrum to give band gap

4.3. Quantitative Analysis

In math, a computation method is used to find an answer in regards to any given problem. The most common computation methods make up the majority of basic math functions including addition, subtraction, multiplication, and division. Computational mathematics involves mathematical research in areas of science where computing plays a central and essential role, emphasizing algorithms, numerical methods, and symbolic computations [10]. Computation in research is prominent. Thus computation method was used to determine the band gap and particles size as described in the sections that follow.

4.3.1. Band Gap Computation

Data used in computing the band gap was the one obtained from the spectrum data. The band gap and particle size of the CdS quantum dots were determined. The following calculation method was used to determine the particle size of the CdS quantum dots. Using the Eq. (4), the cut-off wavelength was determined as [9];

$$\lambda_c = \frac{1.8458}{0.0042/nm} = 439.5\ nm \tag{4}$$

Using the value obtained in Eq. (4), CdS quantum dots the band gap was easily calculated:

$$E_g^{\ *} = \frac{hc}{\lambda_c} = \frac{(6.626\times10^{-34}\,Js)(2.997\times10^{8}\,m/s)}{439.5\times10^{9}\,m}$$

$$E_g^{\ *} = 4.519\times10^{-19}\,J = 2.821\ eV$$

4.3.2. Particle Size Computation

Using the calculated band gap value, many other known constants can be obtained [1, 2, 3,14,15]. The particle size of the quantum dots can be determined from the effective-mass model as expressed in Eq. (1):

$$E_g^{\ *} = E_g^{\ bulk} + \frac{\bar{h}^2\pi^2}{2r^2}\left(\frac{1}{m_e^{\ *}} + \frac{1}{m_h^{\ *}}\right) - \frac{1.8e^2}{4\pi\varepsilon\varepsilon_0 r} - \frac{0.124e^4}{\bar{h}^2(4\pi\varepsilon\varepsilon_0)^2}\left(\frac{1}{m_e^{\ *}} + \frac{1}{m_h^{\ *}}\right)^{-1} \tag{5}$$

where the values of all constants are defined in Eq. (1). This equation can be rearranged to give a quadratic equation as a function of the radius, r [5]:

$$E_g^{\ *}r^2 = E_g^{\ bulk}r^2 + \frac{\bar{h}^2\pi^2}{2}\left(\frac{1}{m_e^{\ *}} + \frac{1}{m_h^{\ *}}\right) - \frac{1.8e^2 r}{4\pi\varepsilon\varepsilon_0} - \frac{0.124e^4}{\bar{h}^2(4\pi\varepsilon\varepsilon_0)^2}\left(\frac{1}{m_e^{\ *}} + \frac{1}{m_h^{\ *}}\right)^{-1} r^2 \tag{6}$$

Implying that;

$$\left[E_g^{\ *} - E_g^{\ bulk} + \frac{0.124e^4}{\bar{h}^2(4\pi\varepsilon\varepsilon_0)^2}\left(\frac{1}{m_e^{\ *}} + \frac{1}{m_h^{\ *}}\right)^{-1}\right]r^2 + \left[\frac{1.8e^2}{4\pi\varepsilon\varepsilon_0}\right]r - \frac{\bar{h}^2\pi^2}{2}\left(\frac{1}{m_e^{\ *}} + \frac{1}{m_h^{\ *}}\right) = 0 \tag{7}$$

To give a quadratic equation simplified as;

$$ar^2 + br + c = 0$$

$$r = \frac{-b \pm \sqrt{b^2 - 4ac}}{2a}$$

In this case, the coefficient, *a*, can be expressed as [6];

$$a = \left[E_g^{\ *} - E_g^{\ bulk} + \frac{0.124e^4}{\bar{h}^2(4\pi\varepsilon\varepsilon_0)^2}\left(\frac{1}{m_e^{\ *}} + \frac{1}{m_h^{\ *}}\right)^{-1}\right] \tag{8}$$

The value of coefficient a, can further is calculated as;

$$a = 4.519\times10^{-19}\,J - 3.88\times10^{-19}\,J +$$

$$\frac{0.124(1.602\times10^{-19}C)^4}{(6.626\times10^{-34}\,Js/2\pi)^2(4\pi(5.7)(8.854\times10^{-12}C^2/Nm^2))^2}\times\left(\frac{1}{0.19(9.11\times10^{-31}kg)} + \frac{1}{0.80(9.11\times10^{-31}kg)}\right)^{-1}$$

$$a = 6.645\times10^{-20}\,J$$

Equally, the coefficient, b, can be calculated from [16];

$$b = \left[\frac{1.8e^2}{4\pi\varepsilon\varepsilon_0}\right] \tag{9}$$

$$b = \frac{1.8(1.602\times10^{-19}C)^2}{4\pi(5.7)(8.854\times10^{-12}C^2/Nm^2)}$$

$$b = 7.284\times10^{-29}\,Jm$$

Finally, the coefficient, c, is equally determined using the expression [11];

$$c = -\frac{\bar{h}^2\pi^2}{2}\left(\frac{1}{m_e^*}+\frac{1}{m_h^*}\right) \quad (10)$$

To give;

$$= \frac{-(6.626\times10^{-34}Js/2\pi)^2\pi^2}{2}\times\left(\frac{1}{0.19(9.11\times10^{-31}kg)}+\frac{1}{0.80(9.11\times10^{-31}kg)}\right)$$

$$c = -3.924\times10^{-37}\,Jm^2$$

Based on the calculated coefficients a, b, and c as determined above, the particle size, r, can be easily be calculated as;

$$r = \frac{-7.284\times10^{-29}Jm \pm \sqrt{(7.284\times10^{-29}Jm)^2 - 4(6.645\times10^{-20}J)(-3.924\times10^{-37}Jm^2)}}{2(6.645\times10^{-20}J)}$$

$$= 1.9nm$$

Hence, twice the size becomes; $2r = 3.8nm$ .The measured particle size, at 3.8 nm was very realistic value. It is on the same order of magnitude as 7.6 nm, and falls within the range given by 3nm to 7 nm, which was produced by a very similar method. Equally, since a shift to the left was caused by the smaller particle size, there was consistency between this investigation and that of related literature [7, 8, 11, 13, 17]. Such a small particle size is expected by this synthesis method, because instead of the synthesis reaction occurring freely in solution, the polar precursors must react in the inside of the inverted micelles [12]. The particle size of 3.8 nm is below the Bohr radius for a CdS quantum dot, which is around 5 nm. As a result, it can be said that quantum confinement will occur for an electron-hole pair or exciton [18] in a quantum dot of this sample.

5. Conclusion

The main objective of this investigation was to measure prepare a sample of CdS quantum dots and obtain a UV-Vis spectrum. The spectrum was to be used to determine the band gap and particle size which was achieved successfully. The principle results of this investigation on sample gave a particle size of around 3.812 nm, with a band gap of 2.812 eV which was consistent with literature. The particle size and band gap were measured easily from the spectrum, giving values that also agreed with literature and theory. It is finally concluded that the synthesis method used gave a high level of quantum dot in a very pure and simple way and the CdS quantum dots produced hold potential for use in materials and devices requiring properties originating from the effect of quantum-confinement.

References

1. Zhao, J., Wu, J., Yu, F., Zhang, X., Lan, Z., & Lin, J. (2013). Improving the photovoltaic performance of cadmium sulfide quantum dots-sensitized solar cell by graphene/titania photoanode. *Electrochimica Acta*, *96*, 110-116.
2. Chen, J. L., & Zhu, C. Q. (2005). Functionalized cadmium sulfide quantum dots as fluorescence probe for silver ion determination. *Analytica Chimica Acta*, *546*(2), 147-153.
3. Zhu, Y., Li, Z., Chen, M., Cooper, H. M., Lu, G. Q. M., & Xu, Z. P. (2013). One-pot preparation of highly fluorescent cadmium telluride/cadmium sulfide quantum dots under neutral-pH condition for biological applications. *Journal of colloid and interface science*, *390*(1), 3-10.

4. Li, K. G., Chen, J. T., Bai, S. S., Wen, X., Song, S. Y., Yu, Q., ... & Wang, Y. Q. (2009). Intracellular oxidative stress and cadmium ions release induce cytotoxicity of unmodified cadmium sulfide quantum dots. *Toxicology in Vitro*, *23*(6), 1007-1013.
5. Santra, P. K., & Kamat, P. V. (2013). Tandem-layered quantum dot solar cells: tuning the photovoltaic response with luminescent ternary cadmium chalcogenides. *Journal of the American Chemical Society*, *135*(2), 877-885.
6. Santra, P. K., & Kamat, P. V. (2013). Tandem-layered quantum dot solar cells: tuning the photovoltaic response with luminescent ternary cadmium chalcogenides. *Journal of the American Chemical Society*, *135*(2), 877-885.
7. Marin, S., & Merkoçi, A. (2009). Direct electrochemical stripping detection of cystic-fibrosis-related DNA linked through cadmium sulfide quantum dots. *Nanotechnology*, *20*(5), 055101.
8. Larson, D. R., Zipfel, W. R., Williams, R. M., Clark, S. W., Bruchez, M. P., Wise, F. W., & Webb, W. W. (2003). Water-soluble quantum dots for multiphoton fluorescence imaging in vivo. *Science*, *300*(5624), 1434-1436.
9. Pham, T. A., Choi, B. C., & Jeong, Y. T. (2010). Facile covalent immobilization of cadmium sulfide quantum dots on graphene oxide nanosheets: preparation, characterization, and optical properties. *Nanotechnology*, *21*(46), 465603.
10. Razvodov, A. A., Nebogatikov, M. S., Shishkina, E. V., & Shur, V. Y. (2013). Sizes and fluorescence of cadmium sulfide quantum dots. *Physics of the Solid State*, *55*(3), 624-628.
11. Stürzenbaum, S. R., Höckner, M., Panneerselvam, A., Levitt, J., Bouillard, J. S., Taniguchi, S., ... & Suhling, K. (2013). Biosynthesis of luminescent quantum dots in an earthworm. *Nature Nanotechnology*, *8*(1), 57-60.
12. Liu, Z., Wu, B., Zhu, Y., Wang, F., & Wang, L. (2013). Cadmium sulphide quantum dots sensitized hierarchical bismuth oxybromide microsphere with highly efficient photocatalytic activity. *Journal of colloid and interface science*, *392*, 337-342.
13. Tang, S., Cai, Q., Chibli, H., Allagadda, V., Nadeau, J. L., & Mayer, G. D. (2013). Cadmium sulfate and CdTe-quantum dots alter DNA repair in zebrafish (Danio rerio) liver cells. *Toxicology and applied pharmacology*, *272*(2), 443-452.
14. Kamat, P. V. (2013). Quantum dot solar cells. The next big thing in photovoltaics. *The Journal of Physical Chemistry Letters*, *4*(6), 908-918.
15. Tang, S., Allagadda, V., Chibli, H., Nadeau, J. L., & Mayer, G. D. (2013). Comparison of cytotoxicity and expression of metal regulatory genes in zebrafish (Danio rerio) liver cells exposed to cadmium sulfate, zinc sulfate and quantum dots. *Metallomics*, *5*(10), 1411-1422.
16. Singh, S., Garg, S., Chahal, J., Raheja, K., Singh, D., & Singla, M. L. (2013). Luminescent behavior of cadmium sulfide quantum dots for gallic acid estimation. *Nanotechnology*, *24*(11), 115602.
17. Shen, Y. J., & Lee, Y. L. (2008). Assembly of CdS quantum dots onto mesoscopic TiO2 films for quantum dot-sensitized solar cell applications. *Nanotechnology*, *19*(4), 045602.
18. Moret, S., Bécue, A., & Champod, C. (2013). Cadmium-free quantum dots in aqueous solution: Potential for fingermark detection, synthesis and an application to the detection of fingermarks in blood on non-porous surfaces. *Forensic science international*, *224*(1), 101-110.

Bibliography

1. Cliff Orori Mosiori is a researcher and doubles up as a lecturer at the Department of Mathematics and Physics, Technical University of Mombasa.
2. E. N. Makori is a PhD student in solid state at the department of Physics of Kenyatta University.
3. Duke Ayetah Oeba is a PhD student in Materials Science for optoelectronic devices at the Department of Physics of Kenyatta University.